COSY AUTHORS

# COSY BOOK-Contribution to Chapter 19

November 3, 1999

Springer-Verlag
Berlin Heidelberg New York
London Paris Tokyo
Hong Kong Barcelona
Budapest

# Table of Contents

# 1. Satellite Attitude Control Problem

Authors:

*Thomas Bak, Mogens Blanke, Rafał Wisniewski*
Aalborg University
Dept. of Control Engineering
Fredrik Bajers Vej. 7, DK–9220 Aalborg
email: bak,blanke,raf@control.auc.dk

*Alessandro Astolfi*
Imperial College
Department of Electrical and Electronic Engineering
Exhibition Road, London SW7-2BT, United Kingdom
email: a.astolfi@ic.ac.uk

*Karlheinz Spindler*
Fachhochschule Wiesbaden
Fachbereich Mathematik, Naturwissenschaften,
Datenverarbeitung und Umwelttechnik,
Kurt-Schumacher-Ring 18, D-65197 Wiesbaden, Germany
email: spindler@r5.mnd.fh-wiesbaden.de

*Pedro Tavares, Paulo Tabuada, Pedro Lima*
Instituto de Sistemas e Robotica
Instituto Superior Tecnico - Torre Norte
Av. Rovisco Pais 1, 1049-001 Lisboa, Portugal
email: pts,pal,tabuada@isr.ist.utl.pt

**Abstract.** The entire concept for the attitude control system is presented in this chapter. Three issues are in the focus: fault tolerant control, attitude control and the attitude determination.

## 1.1 Inroduction to the Attitude Control Problem

$$sdsd \tag{1.1}$$

Many valuable control methods have been developed over the past years since the first satellite was launched in 1957. In these years the subject of attitude control became very mature. Therefore it is not possible to mention in this limited framework all valuable algorithms and techniques published and implemented so far. The contents of this chapter is confined to four issues, which are of interest in the COSY programme: fault tolerant control of Attitude Control System (ACS), environmental disturbance attenuation, slew maneuver, three axis attitude control and attitude determination. The common feature of the methods presented in this chapter is that a spacecraft is considered as a nonlinear object. Unfortunatelly several important issues, which could contribute to completeness of the work are not considered. Here, the topics of orbit determination and control, guidance and navigation are not covered. An interested reader is refered to (Wertz 1990) for more detailes on the design of the entire attitude and orbit control system.

The chapter provides a number of algorithms for solving very specific attitude control problems, which comprise a small part of overall ACS functionality. The ACS likewise the power, the telecommunication, and the mechanical subsystem are serving a payload in fulfilling the mission requirements. The ASC in its work is dependent on the most of the spacecraft subsystems. In order to communicate with other subsystem ACS is capable to send and receive messages to other subsystems and a ground station. Furthermore, it has to be able to read sensor data in each control cycle and to send commands to the actuators. The ACS functionality can be divided into four blocks:

- **Attitude Determination** - used for estimating the rotation (attitude) and the angular velocity often with help of sensor fusion techniques of all available sensors,
- **Attitude Control** - responsible for attitude/angular velocity corrections, comprises the control algorithm for computing torque niveau to the actuators,
- **Fault Detection** used for for detecting the faults, malfunctions in the ACS itself (Attitude Determination, Attitude Control) and ACS dependent subsystems (actuators, sensors),
- **ACS Supervisor** - responsible for making decisions concerning reconfiguration of ACS, communicating with on-board computer, providing autonomy of ACS.

The structure of the chapter is as follows. A model of a rigid body in the central gravitational field is addressed in Section 1.1.1. The motion of the satellite is described by a set of nonlinear ordinary differential equations. Its solution: angular momentum and the satellite rotation remain on a certain manifold. The emphasis in this section is on the attitude representation by a rotation matrix as the element of the special orthogonal group, $SO_3(\mathbb{R})$ and a unit quaternion belonging to $\mathbb{S}^3$ (3-dimentional unit spheres in four dimensional Euclidean space). Section **??** treats an overall architecture of a spacecraft. The work is motivated by the Danish Ørsted satellite. The next four sections are devoted to attitude and rate control. Section **??** discusses two important issues: disturbance attenuation of an under-actuated satellite and output feedback control. An issue of optimal slew maneuver is addressed in Section **??**. The control problem is formulated on the Lie groups, and solved using Pontryagin's Principle modified to an arbitrary manifold. The three axis attitude control for a magnetic actuated satellite is presented in Sections **??** and **??**. Sections **??** considers the problem from a time-varying, nonlinear system point of view and suggests various controllers for three-axis stabilization. Section **??** is a further development of the Lyapunov approach in Section **??** by applying one step ahead prediction of the spacecraft kinetic energy. Proposed control algorithms are successfully implemented for a spinning and a three axis stabilized satellite. The last but not least part of this chapter, Section **??**, is devoted to attitude determination using sensor fusion in an extended Kalman filter.

### 1.1.1 Coordinate Systems

The motion of a spacecraft considered in this chapter is related to four coordinate systems: Principal Coordinate System (PCS), built on the spacecraft principal axes, a Local-Vertical-Local-Horizontal Coordinate System (LVLH) referring to the current position of the satellite in orbit, and an Earth Centered Inertial Coordinate System (ECI), an inertial frame with the origin in the Earth's center of mass. The formal definitions of these coordinate systems are

- **Principal Coordinate System (PCS)** is a right orthogonal coordinate system built on the Spacecraft's principal axes with the origin placed in the center of mass. A vector $\boldsymbol{v}$ resolved in PCS is denoted by $\boldsymbol{v}^{\mathrm{p}}$.
- **Local-Vertical-Local-Horizontal Coordinate System (LVLH)** is a right orthogonal coordinate system with the origin at the spacecraft's center of mass. The z axis (local vertical) is parallel to the radius vector and points from the spacecraft center of mass to the center of the Earth . The positive y axis is pointed in the direction of the negative angular momentum vector. The x axis (local horizontal) completes the right orthogonal coordinate system. The positive x axis lies in the orbital plane in the direction of the velocity vector (only identical to the velocity vector for perfectly circular orbits). A vector $\boldsymbol{v}$ resolved in LVLH is denoted by $\boldsymbol{v}^{\mathrm{o}}$.
- **Earth Centered Inertial Coordinate System (ECI)** is the frame with the origin in the Earth's center. The z axis is parallel to the rotation axis of the Earth and points towards the North Pole. The x axis is parallel to the

line connecting the center of the Earth with Vernal Equinox and points towards Vernal Equinox (Vernal Equinox is the point where the ecliptic crosses the Earth equator going from South to North on the first day of spring). A vector $\boldsymbol{v}$ resolved in ECI is denoted by $\boldsymbol{v}^{\mathrm{i}}$.

**Table 1.1.** Notation

| | |
|---|---|
| $\boldsymbol{\Omega}_{\mathrm{pi}}$ | angular velocity of PCS in ECI, |
| $\boldsymbol{\Omega}_{\mathrm{po}}$ | angular velocity of PCS in LVLH, |
| $\boldsymbol{\Omega}_{\mathrm{oi}}$ | angular velocity of LVLH in ECI, |
| $\omega_{\mathrm{o}}$ | orbital rate, |
| $\mathsf{I}$ | inertia tensor of the satellite, |
| $I_{\mathrm{x}}, I_{\mathrm{y}}, I_{\mathrm{z}}$ | moments of inertia about x-,y- and z-principal axes, |
| $\boldsymbol{N}_{\mathrm{ctrl}}$ | control torque, |
| $\boldsymbol{N}_{\mathrm{gg}}$ | gravity gradient torque, |
| $\boldsymbol{N}_{\mathrm{dist}}$ | disturbance torques, |
| $\boldsymbol{m}$ | magnetic moment generated by a set of the coils, |
| $\boldsymbol{B}$ | magnetic field of the Earth, |
| ${}^{\mathrm{p}}_{\mathrm{o}}\boldsymbol{q}$ | quaternion representing rotation of PCS in LVLH, |
| $\boldsymbol{q}, q_4$ | vector part and scalar part of ${}^{\mathrm{p}}_{\mathrm{o}}\boldsymbol{q}$, |
| $\mathsf{A}({}^{\mathrm{c}}_{\mathrm{o}}\boldsymbol{q})$ | attitude matrix based on ${}^{\mathrm{c}}_{\mathrm{o}}\boldsymbol{q}$, |
| $\boldsymbol{i}_{\mathrm{o}}, \boldsymbol{j}_{\mathrm{o}}, \boldsymbol{k}_{\mathrm{o}}$ | unit vectors along x-, y-, z-axis of LVLH, |
| $n_{\mathrm{coil}}$ | number of coil windings, |
| $i_{\mathrm{coil}}(t)$ | current in coil, |
| $A_{\mathrm{coil}}$ | coil area, |
| $\mathsf{E}_{\mathrm{n}}$ | n by n identity matrix. |

**List of Symbols.**

### 1.1.2 Equations of Motion

Motion of a spacecraft is described by a set of nonlinear ordinary differential equations. Its solution: angular momentum and the satellite orientation remain on a certain manifold. This motion can be described with respect to a reference coordinate systems, which are fixed or revoluting in the inertial frame. The spacecraft is considered as a rigid body which orientation is corrected to a reference frame by a feedback system.

The mathematical model of a satellite is described by well-known dynamic and the kinematic equations of motion, see e.g. (Hughes 1986) or (Wertz 1990). The kinematics characterizes relation between satellite's angular velocity and its orientation in space, the attitude. The minimum number of parameters locally identifying the attitude is three (Euler angles), however, four parameters are necessary for global attitude representation (a unit quaternion). The dynamics describes dependence between external torques and the spacecraft's angular velocity. The external torques are disturbances and a control torque.

### 1.1.3 Attitude Parameterization

The fundamental problem of the attitude representation is to specify an orientation of a coordinate system fixed in a spacecraft {s} with respect to a reference coordinates {r}. The orientation can be parameterized by several methods: a rotation matrix, a unit quaternion, Euler angles, a Gibbs vector. The most natural attitude description is given by the rotation matrix, which is composed of a unit vectors of {s} projected on {r}. This representation uses nine components with 6 constrains, thus the attitude can be locally specified by three parameters. The Euler angles seems to be most physically appealing three parameter representation of attitude. The minimum number of parameters necessary to give a global representation is four. For this purpose a unit quaternion can be used, which consists of four components with an amplitude constraint.

### 1.1.4 Rotation Matrix

Consider a triad of unit vectors spanning the coordinate system {r}, and call them $\boldsymbol{i}_{\mathrm{r}}$, $\boldsymbol{j}_{\mathrm{r}}$, and $\boldsymbol{k}_{\mathrm{r}}$. The relations between these vector are

$$\boldsymbol{i}_{\mathrm{r}} \times \boldsymbol{j}_{\mathrm{r}} = \boldsymbol{k}_{\mathrm{r}}, \quad \boldsymbol{j}_{\mathrm{r}} \times \boldsymbol{k}_{\mathrm{r}} = \boldsymbol{i}_{\mathrm{r}} \text{ and } \boldsymbol{k}_{\mathrm{r}} \times \boldsymbol{i}_{\mathrm{r}} = \boldsymbol{j}_{\mathrm{r}}. \tag{1.2}$$

The basic problem is now to describe the orientation of this triad relative the coordinate system {s}. This orientation is characterized completely by specifying the components of $\boldsymbol{i}_{\mathrm{r}}$, $\boldsymbol{j}_{\mathrm{r}}$, and $\boldsymbol{k}_{\mathrm{r}}$ along the x, y and z axes of {s}: $(\boldsymbol{i}_{\mathrm{r}})_{\mathrm{s}}$, $(\boldsymbol{j}_{\mathrm{r}})_{\mathrm{s}}$, $(\boldsymbol{k}_{\mathrm{r}})_{\mathrm{s}}$. Compose these components into the following 3 by 3 matrix

$$\mathsf{A} = \left[(\boldsymbol{i}_{\mathrm{r}})_{\mathrm{s}} \quad (\boldsymbol{j}_{\mathrm{r}})_{\mathrm{s}} \quad (\boldsymbol{k}_{\mathrm{r}})_{\mathrm{s}}\right] \tag{1.3}$$

The matrix $\mathsf{A}$ maps vectors from the coordinate system {r} to {s} and it is known as the rotation matrix.

There are six constraints imposed on the rotation matrix $\mathsf{A}$. The first three comes from the fact the the length of vectors $\boldsymbol{i}_{\mathrm{r}}$, $\boldsymbol{j}_{\mathrm{r}}$, $\boldsymbol{k}_{\mathrm{r}}$ is one. The remaining three are due to mutual orthogonality of the triad, Eq. (1.2). These constraints in the language of the matrix product can be summarized in equation

$$\mathsf{A}\mathsf{A}^{\mathrm{T}} = \mathsf{A}^{\mathrm{T}}\mathsf{A} = \mathsf{E}. \tag{1.4}$$

It means that the rotation matrix is an orthogonal matrix with the following properties, see (**?**)

1. for any column n-vector $\boldsymbol{v}$, $\| \mathsf{A}\boldsymbol{v} \| = \| \boldsymbol{v} \|$,
2. for any n-vectors $\boldsymbol{v}$ and $\boldsymbol{w}$, $\langle \mathsf{A}\boldsymbol{v}, \mathsf{A}\boldsymbol{w} \rangle = \langle \boldsymbol{v}, \boldsymbol{w} \rangle$, where $\langle \ , \ \rangle$ denotes the inner product in $\mathbb{R}^{\mathrm{n}}$.
3. $\det \mathsf{A} = \langle \boldsymbol{i}_{\mathrm{r}}, (\boldsymbol{j}_{\mathrm{r}} \times \boldsymbol{k}_{\mathrm{r}}) \rangle = 1$.

The rotation matrix can be represented as the exponential of an antisymmetric matrix

$$\mathsf{A} = \exp(\psi_1 \mathsf{E}_1 + \psi_2 \mathsf{E}_2 + \psi_2 \mathsf{E}_3), \tag{1.5}$$

where

$$\boldsymbol{E}_1 := \begin{bmatrix} 0 & 0 & 0 \\ 0 & 0 & 1 \\ 0 & -1 & 0 \end{bmatrix}, \qquad \boldsymbol{E}_2 := \begin{bmatrix} 0 & 0 & -1 \\ 0 & 0 & 0 \\ 1 & 0 & 0 \end{bmatrix}, \qquad \boldsymbol{E}_3 := \begin{bmatrix} 0 & 1 & 0 \\ -1 & 0 & 0 \\ 0 & 0 & 0 \end{bmatrix} \tag{1.6}$$

The vector $\boldsymbol{\Psi} = \begin{bmatrix} \psi_1 & \psi_2 & \psi_3 \end{bmatrix}^{\mathrm{T}}$ is interpreted as a product of the angle of rotation, $\psi$ and the axis of rotation, $\boldsymbol{\epsilon}$, $\boldsymbol{\Psi} = \psi\boldsymbol{\epsilon}$. Eq. (1.5) is often represented in more compact form involving the following isomorphism

$$\mathsf{S} : \boldsymbol{v} \mapsto \begin{bmatrix} 0 & v_3 & -v_2 \\ -v_3 & 0 & v_1 \\ v_2 & -v_1 & 0 \end{bmatrix}, \tag{1.7}$$

namely $\mathsf{A} = \exp\left(\mathsf{S}(\boldsymbol{\Psi})\right)$.

It is worth mentioning that the axis of rotation $\boldsymbol{\epsilon}$ coincides with the eigenvector of $\mathsf{A}$ corresponding to the eigenvalue equal 1. The angle of rotation and the components of the axis of rotation can be calculated using the Rodriques formula, (**?**)

$$\cos\psi = \frac{1}{2}\left(\mathrm{tr}(\mathsf{A}) - 1\right), \qquad \boldsymbol{\epsilon} = \frac{1}{2\sin\psi} \begin{bmatrix} A_{23} - A_{32} \\ A_{31} - A_{13} \\ A_{12} - A_{21} \end{bmatrix}. \tag{1.8}$$

The kinematic equation is the derivative of the rotation matrix $\mathsf{A}$ with respect to time

$$\frac{d\mathsf{A}}{dt} = \lim_{\Delta t \to 0} \frac{\mathsf{A}(t + \Delta t) - \mathsf{A}(t)}{\Delta t} = \mathsf{S}(\boldsymbol{\Omega})\ \mathsf{A}. \tag{1.9}$$

The vector $\boldsymbol{\Omega}$ lies along axis of the infinitesimal rotation occurring between $t$ and $t + \delta t$. This direction is known as instantaneous axis of rotation.

The final but very important remark is that the rotation matrices form a special orthogonal group $\mathrm{SO}_3(\mathbb{R})$. For attitude control purpose $\mathrm{SO}_3(\mathbb{R})$ can be considered as a Lie group with its Lie algebra $so_3(\mathbb{R})$ consisting of 3 by 3 real antisymmetric matrices (with basis $\mathsf{E}_1, \mathsf{E}_2, \mathsf{E}_3$). The dynamic system described by Eq. (1.9) is right invariant meaning that the vector field for each group element, $\mathsf{A}$ is determined by its value at the identity, (**?**), here given by simple multiplication by $\mathsf{A}$ on the right hand side of Eq. (1.9). Further details concerning the attitude control problem on Lie groups will be considered in Section **??**.

### 1.1.5 Unit Quaternion

Consider a four dimensional Euclidean space, $\mathbb{E}^4$, and let $\boldsymbol{e}$ denote a unit vector in $\mathbb{E}^4$, and let $\mathbb{E}$ be an orthogonal complement to the vector space spanned by $\boldsymbol{e}$. Now, any vector $\tilde{\boldsymbol{q}}$ in $\mathbb{E}^4$ can be uniquely expressed as

$$\tilde{\boldsymbol{q}} = q_0\boldsymbol{e} + \boldsymbol{q}, \tag{1.10}$$

where $q_0 \in \mathbb{R}$, and $\boldsymbol{q} \in \mathbb{E}$.

$\mathbb{E}$ is three dimensional and every vector can be represented as a linear combination of the triad of mutually perpendicular unit vectors $\boldsymbol{i}, \boldsymbol{j}, \boldsymbol{k}$. Therefore, an element of $\mathbb{E}^4$ is given by

$$\tilde{\mathbf{q}} = q_0\boldsymbol{e} + q_1\boldsymbol{i} + q_2\boldsymbol{j} + q_3\boldsymbol{k}. \tag{1.11}$$

Now a definition from (**?**) of a quaternion can be adopted. Quaternions are elements of $\mathbb{E}^4$ endowed with the vector structure of $\mathbb{E}^4$ and the multiplication

$$\tilde{\boldsymbol{q}}\tilde{\boldsymbol{s}} = (q_0 s_0 - \langle \boldsymbol{q}, \boldsymbol{s}\rangle)\boldsymbol{e} + q_0\boldsymbol{s} + s_0\boldsymbol{q} + \boldsymbol{q} \times \boldsymbol{s} \tag{1.12}$$

for any $\tilde{\boldsymbol{q}} = q_0\boldsymbol{e} + \boldsymbol{q}$ and $\tilde{\boldsymbol{s}} = s_0\boldsymbol{e} + \boldsymbol{s}$

The construction of the unit quaternion arises from the Euler's theorem that the general displacement of a rigid body with one point fixed is a rotation about some axis. Thus, the rotation of coordinate systems can be uniquely described by a unit vector, $\boldsymbol{\epsilon}$, the axis of rotation, and the angle of rotation $\psi$. A unit quaternion, $\tilde{\boldsymbol{q}}$ can be interpreted as a combination of the components of the unit vector and the angle of rotation in the following formula

$$\tilde{\boldsymbol{q}} = \cos\frac{\psi}{2}\boldsymbol{e} + \sin\frac{\psi}{2}\boldsymbol{\epsilon}, \tag{1.13}$$

Notice that the same attitude can be described by two different unit quaternions $\mathbf{q}$ and $-\mathbf{q}$, the first is given for the angle of rotation $\phi$, and the latter for the angle $2\pi + \phi$.

Now kinematic equation is formulated as

$$\frac{d\tilde{\boldsymbol{q}}}{dt} = \frac{1}{2}\tilde{\boldsymbol{\Omega}}\,\tilde{\boldsymbol{q}}, \tag{1.14}$$

where $\tilde{\boldsymbol{\Omega}} = 0\boldsymbol{e} + \boldsymbol{\Omega}$, is the quaternionic representation of the instantaneous angular velocity.

### 1.1.6 Kinematics of LEO Spacecraft

The general forms for kinematics of a rotating body were derived in the last two subsections. The kinematics for a LEO satellite is provided in this subsection. In fact, the only difference is that the coordinate system PCS takes place of $\{s\}$ and LVLH takes place of $\{r\}$, thus for instance the quaternionic kinematics is

$$\frac{\mathrm{d}}{\mathrm{dt}} {}^p_o\tilde{\boldsymbol{q}} = \frac{1}{2} \tilde{\boldsymbol{\Omega}}_{\mathrm{po}} \, {}^p_o\tilde{\boldsymbol{q}}, \tag{1.15}$$

where ${}^p_o\tilde{\boldsymbol{q}}$ is the unit quaternion describing rotation from LVLH to PCS, $\boldsymbol{\Omega}_{\mathrm{po}}$ is the angular velocity of PCS in LVLH. It is sometimes convenient to represent Eq. (1.15) by an equivalent formula expressed by separate integrations of the vector and the scalar part of the quaternion

$$\begin{aligned} \dot{q}_0 &= -\frac{1}{2}\boldsymbol{\Omega}_{\mathrm{po}}\boldsymbol{q}, \\ \dot{\boldsymbol{q}} &= \frac{1}{2}\boldsymbol{\Omega}_{\mathrm{po}}q_0 - \frac{1}{2}\boldsymbol{\Omega}_{\mathrm{po}} \times \mathbf{q}. \end{aligned} \tag{1.16}$$

The dynamics of a rigid body addressed in the next section corresponds the spacecraft rotation in an inertial coordinate system, therefore it is necessary to state en explicit formula for relation between $\boldsymbol{\Omega}_{\mathrm{po}}$ and $\boldsymbol{\Omega}_{\mathrm{pi}}$. The rotation of LVLH in ECI is about the axis normal to the orbital plane in the direction of $-\boldsymbol{j}_{\mathrm{o}}$. The rate of this rotation has the magnitude $\omega_{\mathrm{o}}$ - here we made an approximation that the orbital plane is invariant, i.e. motion of line of nodes is disregarded

$$\boldsymbol{\Omega}_{\mathrm{po}} = \boldsymbol{\Omega}_{\mathrm{pi}} - \boldsymbol{\Omega}_{\mathrm{oi}} = \boldsymbol{\Omega}_{\mathrm{pi}} + \omega_{\mathrm{o}}(t)\boldsymbol{j}_{\mathrm{o}}. \tag{1.17}$$

### 1.1.7 Dynamics of LEO Spacecraft

The rotational motion about the center of mass is described by the direct Newtonian approach. The solution is a set of three differential equations known as Euler's equation of motion. The dynamics relates torques acting on the spacecraft to the satellite's angular momentum. The Euler's equation in the inertial coordinates, ECI, is the well known formula

$$\left(\frac{\mathrm{d}\boldsymbol{L}}{\mathrm{d}t}\right)_{\mathrm{i}} = \boldsymbol{N}_{\mathrm{i}}, \tag{1.18}$$

where $\boldsymbol{N}$ is the sum of external torques acting on the body, $\boldsymbol{L}$ is the angular momentum, the subscript i is used because the derivative is with respect to ECI. The angular momentum is defined as

$$\boldsymbol{L} = \mathsf{I}\boldsymbol{\Omega}_{\mathrm{pi}}, \tag{1.19}$$

where $\mathsf{I}$ is the inertia tensor, its elements are the inertia coefficients. The inertia tensor has a remarkably convenient form in PCS. In PCS the coordinates are spanned on the spacecraft's principal axes, and the inertia tensor is a diagonal 3 by 3 matrix. The derivative in Eqs. (1.18) can be represented in body fixed coordinates

$$\frac{d}{dt}\boldsymbol{L}_{\mathrm{p}} = \mathsf{S}(\boldsymbol{\Omega}_{\mathrm{pi}})\boldsymbol{L}_{\mathrm{p}} + \left(\frac{d}{dt}\boldsymbol{L}_{\mathrm{i}}\right)_{\mathrm{p}} = \mathsf{S}(\boldsymbol{\Omega}_{\mathrm{pi}})\boldsymbol{L}_{\mathrm{p}} + \boldsymbol{N}_{\mathrm{p}} \tag{1.20}$$

Now, the dynamic equation of motion for a rigid spacecraft in LEO is

$$\mathsf{I}\dot{\boldsymbol{\Omega}}_{\mathrm{pi}}(t) = -\boldsymbol{\Omega}_{\mathrm{pi}}(t) \times \mathsf{I}\boldsymbol{\Omega}_{\mathrm{pi}}(t) + \boldsymbol{N}_{\mathrm{ctrl}}(t) + \boldsymbol{N}_{\mathrm{gg}}(t) + \boldsymbol{N}_{\mathrm{dis}}(t). \tag{1.21}$$

In the equation above the subscript p is dropped. $\boldsymbol{N}_{\mathrm{ctrl}}(t)$ is the control torque, $\boldsymbol{N}_{\mathrm{gg}}(t)$ is the gravity gradient torque and $\boldsymbol{N}_{\mathrm{dis}}(t)$ is the disturbance torques.

**Magnetic torque.** Magnetic control torque is generated by an interaction of the geomagnetic field with the magnetorquer current $i(t)$ which gives rise to a magnetic moment $m(t)$

$$m(t) = n_{coil}\ i_{coil}(t)\ A_{coil}. \tag{1.22}$$

The control torque acting on the satellite is then

$$\boldsymbol{N}_{\mathrm{ctrl}}(t) = \boldsymbol{m}(t) \times \boldsymbol{B}(t), \tag{1.23}$$

where $\boldsymbol{B}(t)$ is the magnetic flux vector of the Earth. The magnetic moment, $\boldsymbol{m}$, is considered as the control signal.

**Gravitational Torque.** Gravitational torque is fundamental component for the model of a LEO spacecraft motion. The gravitational field in space is not uniform, therefore the gravitational forces acting on specific parts of the spacecraft construction are different. Integration of this effects over the whole body gives the gravitational torque, (Hughes 1986)

$$\boldsymbol{N}_{\mathrm{gg}} = \frac{3\mu}{R_{\mathrm{cm}}^3}(\boldsymbol{R}_{\mathrm{cm}} \times \mathsf{I}^c\boldsymbol{R}_{\mathrm{cm}}), \tag{1.24}$$

where $\mu$ is the Earth gravitational constant, $R_{\mathrm{cm}}$ is the distance from the center of the Earth to the spacecraft's center of gravity ($R_{\mathrm{cm}}$ is a subject of variation, when an elliptic orbit is considered), $\boldsymbol{R}_{\mathrm{cm}}$ is the unit vector from the center of the Earth to the spacecraft's center of mass, nadir. Observe that nadir is equivalent to the unit vector on the z axis of LVLH, $\boldsymbol{k}_{\mathrm{o}}$, and the constant $\frac{\mu}{R_{cm}^3} = \omega_{\mathrm{o}}^2$, where $\omega_{\mathrm{o}}$ is the orbital rate. Now, the gravitational torque is

$$\boldsymbol{N}_{\mathrm{gg}} = 3\omega_o^2(\boldsymbol{k}_{\mathrm{o}} \times \mathsf{I}\ \boldsymbol{k}_{\mathrm{o}}). \tag{1.25}$$

## 1.2 An Architecture for Fault-tolerant Control of a Small Satellite

## 1.3 Recent Results on Attitude Stabilization

## 1.4 New results on the stabilization of the angular velocity of a rigid body

## 1.5 Optimal Slew Maneuvers Via Geometric Control Theory

## 1.6 Attitude Control using Magnetorquers as Sole Actuators

## 1.7 Predictive Attitude Control of Small Satellites

The attitude control problem of small satellites through geomagnetic field interaction is a particularly challenging problem since magnetic actuaction introduces a non-holonomic constraint on the system: the control torque (1.23) is always perpendicular to the geomagnetic field. The time-varying nature of the problem is also revealed in this equation, the direction parallel to the geomagnetic field is not controllable, however, the geomagnetic field changes along the orbit. This implies that, e.g., yaw is not controllable over the poles but only a quarter of orbit later, i.e., approximately over the equator. Those characteristics must be adequately explored to properly regulate the satellite's attitude. A time-varying predictive algorithm[1] to determine the control moment, which takes advantage of the geomagnetic field changes, is proposed as a solution to this control problem.

Several researchers have approached the attitude control of LEO small satellites. (Ong 1992) proposes some intuitive control laws to tackle this problem, (Steyn 1994) uses a Fuzzy Logic approach that achieves better results than a Linear Quadratic Regulator (LQR), despite considering the constraint of actuating on a single coil at each actuation time. Sliding mode and energy-based solutions are proposed by (Wisniewski 1997) achieving better results than LQRs based on linear periodic theory.

### 1.7.1 Geometry of Solutions

Before solving the problem of attitude stabilization it is important to know if there are solutions and what is the geometry of the solution set. To do so, we start by imposing a natural constraint (stability) on $\boldsymbol{N}_{ctrl}$. Using the satellite total energy as a Lyapunov candidate function (Wisniewski 1997) shows that its time derivative is given by $\dot{E}_{\mathrm{tot}} = \boldsymbol{\Omega}_{\mathrm{po}}^{\mathrm{T}} \boldsymbol{N}_{\mathrm{ctrl}}$. $\dot{E}_{tot} = 0$ represents all the control torques that lie on a plane that is perpendicular to $\boldsymbol{\Omega}_{\mathrm{po}}$. Therefore, imposing $\dot{E}_{tot} < 0$ is the same as constraining the control torque to lie "behind" the plane perpendicular to $\boldsymbol{\Omega}_{\mathrm{po}}$. Furthermore, the control torque is obtained from (1.23), therefore, it must always be perpendicular to the geomagnetic field. As such, the solution of this control problem must satisfy:

$$\left\{ \begin{array}{lcl} \boldsymbol{\Omega}_{\mathrm{po}}^{\mathrm{T}} \boldsymbol{N}_{\mathrm{ctrl}} & < & 0 \\ \boldsymbol{B}^{\mathrm{T}} \boldsymbol{N}_{\mathrm{ctrl}} & = & 0 \end{array} \right. \tag{1.26}$$

It can be seen from (1.26) that the space of solutions is diffeomorphic to $H^2 = \{(x_1, x_2) \in \mathbb{R}^2 \ : \ x_2 > 0\}$ in the general case, or it doesn't exist if $\boldsymbol{\Omega}_{\mathrm{po}}$ is parallel to $\boldsymbol{N}_{\mathrm{ctrl}}$. This is equivalent to state that the solutions to this control problem are infinite in the general case, suggesting a control algorithm that should choose the optimum magnetic moment (or at least the best one, given all the constraints) at each actuation instant, to take advantage of the

[1] This work was supported by PRAXIS/3/3.1/CTAE/1942/95. The authors would like to acknowledge the ESF COSY Programme for supporting a visit of one of the authors to Aalborg University.

particular angular velocity and geomagnetic field. This approach differs from most other solutions available in the literature, which use the same control law for all configurations of the state variables.

### 1.7.2 The Predictive Algorithm

We start by using the kinetic energy as a cost function:

$$J = E_{kin} = \frac{1}{2}\,\boldsymbol{\Omega}_{\mathrm{po}}^{\mathrm{T}}\mathsf{J}\,\boldsymbol{\Omega}_{\mathrm{po}} \tag{1.27}$$

More insight will be given regarding the choice of the cost function when studying the algorithm stability in 1.7.3.

The dynamic model of the satellite is well known and understood, so it can be used to predict the influence of the magnetic moment on the angular velocity. After some straightforward algebra (Paulo Tabuada and Lima 1999) the angular velocity evolution produced by a given control torque can be predicted by:

$$\begin{aligned}\frac{\boldsymbol{\Omega}_{\mathrm{po}}(t+\Delta t)-\boldsymbol{\Omega}_{\mathrm{po}}(t)}{\Delta t} &\simeq \mathsf{J}^{-1}(\mathsf{J}\boldsymbol{\Omega}_{\mathrm{pi}}(t)\times\boldsymbol{\Omega}_{\mathrm{pi}}(t))+\omega_{\mathrm{o}}\boldsymbol{j}_{\mathrm{o}}(t)\times\boldsymbol{\Omega}_{\mathrm{po}}(t)\\ &+ \mathsf{J}^{-1}\boldsymbol{N}_{\mathrm{gg}}(t)+\mathsf{J}^{-1}\boldsymbol{N}_{\mathrm{ctrl}}(t)\end{aligned} \tag{1.28}$$

which may be written as[2]:

$$\begin{aligned}\boldsymbol{\Omega}_{\mathrm{po}}(t+\Delta t) &= \boldsymbol{\Omega}_{\mathrm{po}}(t)+\Delta t f(t)+O((\Delta t)^2)\\ f(t) &= \mathsf{J}^{-1}(\mathsf{J}\boldsymbol{\Omega}_{\mathrm{pi}}\times\boldsymbol{\Omega}_{\mathrm{pi}})+\omega_{\mathrm{o}}\boldsymbol{j}_{\mathrm{o}}\times\boldsymbol{\Omega}_{\mathrm{po}}+\\ &\quad+\mathsf{J}^{-1}\boldsymbol{N}_{\mathrm{gg}}+\mathsf{J}^{-1}\boldsymbol{N}_{\mathrm{ctrl}}\end{aligned} \tag{1.29}$$

and the prediction equation is obtained by discarding the higher order terms:

$$\hat{\boldsymbol{\Omega}}_{\mathrm{po}}(t+\Delta t)=\boldsymbol{\Omega}_{\mathrm{po}}(t)+\Delta t f(t) \tag{1.30}$$

where $\hat{\boldsymbol{\Omega}}_{\mathrm{po}}$ is the predicted angular velocity. It can be seen from Eq. (1.30) that it is possible to predict the effect that a given control torque will produce on the angular velocity. For this prediction one only needs to know the current angular velocities and attitude, the estimates of which are readily available from the attitude determination system (see for example this chapter's last section). Using the prediction equation (1.30) and Eq. (1.23) it is possible to choose from the available magnetic moments the one that minimizes the cost function (1.27), once the geomagnetic field value is available from the magnetometers.

[2] Recall that Eq. (1.29) corresponds to the Euler method for numerically solving first order differential equations.

### 1.7.3 Stability Study

The total energy of satellite is composed of a kinetic term and a potential term, $E_{\text{total}} = E_{\text{kin}} + E_{\text{pot}}$.

Their sum, the total energy, may be considered constant, since the dissipative forces and torques actuating on a satellite are very weak. By dissipating the kinetic energy, the total energy is also decreased. Since the system is not fully controllable it is not possible to place the satellite in a zero kinetic energy configuration and keep it there because gravity-gradient torques will impose a libration movement converting potential energy to kinetic energy. Should all kinetic energy be dissipated by the predictive algorithm, the only stable configuration for the satellite would be a minimum total energy one (${}^{\mathrm{p}}\boldsymbol{k}_{\mathrm{o}} = \pm{}^{\mathrm{o}}\boldsymbol{k}_{\mathrm{o}}$). To show that the proposed algorithm is indeed globally uniformly asymptotically stable we will show that the predictive algorithm induces the negativity of the total energy derivative. The algorithm will choose a control torque ($\boldsymbol{N}^*_{\text{ctrl}}$) that minimizes the estimate of the kinetic energy, that is:

$$\begin{aligned} & \forall\, \boldsymbol{N}_{\text{ctrl}} \quad \hat{J}_{\boldsymbol{N}^*_{\text{ctrl}}}(t+\Delta t) \le \hat{J}_{\boldsymbol{N}_{\text{ctrl}}}(t+\Delta t) \\ \Leftrightarrow \quad & \forall\, \boldsymbol{N}_{\text{ctrl}} \quad \hat{J}_{\boldsymbol{N}^*_{\text{ctrl}}}(t+\Delta t) - J(t) \le \hat{J}_{\boldsymbol{N}_{\text{ctrl}}}(t+\Delta t) - J(t) \end{aligned} \tag{1.31}$$

Since $J(t+\Delta t) = \hat{J}(t+\Delta t) + O((\Delta t)^2)$ Eq. (1.31) can be written as:

$$\forall\, \boldsymbol{N}_{\text{ctrl}}\ J_{\boldsymbol{N}^*_{\text{ctrl}}}(t+\Delta t) - J(t) - O(\Delta t^2) \le J_{\boldsymbol{N}_{\text{ctrl}}}(t+\Delta t) - J(t) - O(\Delta t^2) \tag{1.32}$$

and if we act fast enough:

$$\begin{aligned} & \forall\, \boldsymbol{N}_{\text{ctrl}} \quad \lim_{\Delta t \to 0} \frac{J_{\boldsymbol{N}^*_{\text{ctrl}}}(t+\Delta t) - J(t)}{\Delta t} - \frac{O(\Delta t^2)}{\Delta t} \\ & \le \quad \lim_{\Delta t \to 0} \frac{J_{\boldsymbol{N}_{\text{ctrl}}}(t+\Delta t) - J(t)}{\Delta t} - \frac{O(\Delta t^2)}{\Delta t} \\ \Leftrightarrow \quad & \forall\, \boldsymbol{N}_{\text{ctrl}} \quad \dot{J}_{\boldsymbol{N}^*_{\text{ctrl}}} \le \dot{J}_{\boldsymbol{N}_{\text{ctrl}}} \end{aligned} \tag{1.33}$$

This means that the minimization of (1.27) induces the minimization of the kinetic energy time derivative. And since at each time step where the minimization is performed we have:

$$\frac{\partial \dot{E}_{kin}}{\partial\, \boldsymbol{N}_{\text{ctrl}}} = \frac{\partial \dot{E}_{total}}{\partial\, \boldsymbol{N}_{\text{ctrl}}} - \frac{\partial \dot{E}_{pot}}{\partial\, \boldsymbol{N}_{\text{ctrl}}} \tag{1.34}$$

and $\frac{\partial \dot{E}_{pot}}{\partial\, \boldsymbol{N}_{\text{ctrl}}} = 0$ the control torque that minimizes $\dot{E}_{kin}$ also minimizes $\dot{E}_{total}$ (although $\dot{E}_{kin} \neq \dot{E}_{total}$), this justifies the choice of (1.27). As was shown in 1.7.1, there always exist solutions that guarantee $\dot{E}_{total} < 0$ (except when $\boldsymbol{\Omega}_{\text{po}}$ is parallel to $B$), and the predictive algorithm chooses the one of minimum $\dot{E}_{total}$. We can conclude therefore that $\dot{E}_{total} \le 0$.

So far we have only shown that the system is globally stable, but not asymptotically stable. To show asymptotic stability we realize that ${}^{p}\boldsymbol{m}$ is computed based on the current angular velocity and geomagnetic field, so $\boldsymbol{m} = g(\boldsymbol{\Omega}_{\mathrm{po}}, \boldsymbol{B}(t))$ and therefore the dynamic equation is periodic with the same period of the satellite's orbit. Using a periodic extension to the Lyapunov stability theory due to Krasovskii-LaSalle (Krasovskii 1963) we can show that the system is indeed globally uniformly asymptotically stable towards the reference $\boldsymbol{\Omega}_{\mathrm{po}} = [\ 0 \quad 0 \quad 0\ ]^{\mathrm{T}}$, ${}^{\mathrm{p}}\boldsymbol{k}_{\mathrm{o}} = \pm{}^{\mathrm{o}}\boldsymbol{k}_{\mathrm{o}}$. The proof is similar to the one in (Wisniewski 1997) and will not be repeated here.

### 1.7.4 Simulation Results

PoSAT-1, as other micro-satellites, has reduced control capabilities due to the limited nature of its actuators. The magnetorquer used is composed of three wire coils along the satellite geometrical axes. The attitude control loop sampling period is 10 s and during this time each coil may be fired (one at a time) for up to 3 s with positive or negative polarity and 0.1 s resolution. When the coil is fired, the amplitude of the current that flows through the coil is constant. The resulting control torque is obtained by electromagnetic interaction with the geomagnetic field $\boldsymbol{B}$ as given by Eq. (1.23). The time resolution of the actuator is set to 1 s as a tradeoff between the dimension of the search space (i.e., the number of possible magnetic moment vectors) and control accuracy. Special techniques may also be used to further reduce the search space (e.g. discarding vectors approximately parallel to $\boldsymbol{B}$).

The results presented do not consider disturbance torques such as aerodynamic drag or solar pressure due to the altitude of PoSat-1's orbit (around 800 Km). Simulations were performed for attitude and spin control, where the cost function used was a variation of Eq. (1.27), replacing $\boldsymbol{\Omega}_{\mathrm{po}}$ with $\underset{\mathrm{ref}}{\boldsymbol{\Omega}} = \boldsymbol{\Omega}_{\mathrm{po}} - [\ 0 \quad 0 \quad \omega_{\mathrm{spin}}\ ]^{\mathrm{T}}$.

As can be seen in Eq. (1.29) the controller requires knowledge of the parameters $\boldsymbol{\Omega}_{\mathrm{pi}}$, $\boldsymbol{\Omega}_{\mathrm{po}}$, $\boldsymbol{i}_{\mathrm{o}}$, $\omega_{\mathrm{o}}$ and $\boldsymbol{N}_{\mathrm{gg}}$. To determine the benchmark for controller performance, a perfect knowledge of attitude information was assumed, disregarding the fact that this is a commodity not readily available in the real system, except through the use of an attitude estimator, see for example Section **??**.

Table 1.7.4 presents the results of the two spin tests totaling 200 orbits where twenty different sets of simulation parameters were used. These are divided into de-libration (test A) and spin control (test B). In the first of these two tests the initial simulation values are[3] $\gamma = 60^{o}$, $\boldsymbol{\Omega}_{\mathrm{po}} = [\ 0 \quad 0 \quad 0.02\ ]^{\mathrm{T}}$ and the desired reference is $\gamma = 0^{o}$, $\boldsymbol{\Omega}_{\mathrm{po}} = [\ 0 \quad 0 \quad 0.02\ ]^{\mathrm{T}}$. In the second test the initial values are $\gamma = 0^{o}$, $\boldsymbol{\Omega}_{\mathrm{po}} = [\ 0 \quad 0 \quad 0\ ]^{\mathrm{T}}$ and the desired reference is $\gamma = 0^{o}$, $\boldsymbol{\Omega}_{\mathrm{po}} = [\ 0 \quad 0 \quad 0.02\ ]^{\mathrm{T}}$. The roll angle and starting

[3] Gamma ($\gamma$) is defined as the angle between ${}^{p}\boldsymbol{k}_{o}$ and ${}^{o}\boldsymbol{k}_{o}$.

date/time of the 10 simulations on each batch are randomly distributed in their respective ranges.

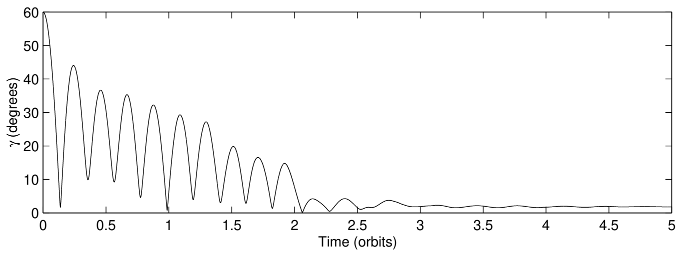


Fig. 1: Gamma plot for simulation number 7 of Test A.

The second column of Table 1.7.4 shows the settling time ($t_s$) of $\gamma$ to $5^o$. Column three shows the pointing accuracy of this angle after ten orbits ($\simeq 6 \times 10^4$ seconds). Column four shows the angular velocity vector norm accuracy after ten orbits and the last column shows the energy spent by the magnetorquer.

| Test A | $t_s$ $(\gamma \leq 5^o)$ | $\gamma$ acc. | $\|{}^p\boldsymbol{\Omega}_{\text{po}}\|$ acc. | Energy spent |
|---|---|---|---|---|
| Mean | 3.2153 | 1.8897 | $5.6913 \times 10^{-5}$ | $2.9921 \times 10^5$ |
| Std. dev. | 1.7288 | 0.26411 | $4.9569 \times 10^{-5}$ | $3.9894 \times 10^4$ |
| Worst case | 6.2061 | 2.2199 | $1.6367 \times 10^{-4}$ | $3.9541 \times 10^5$ |
| Units | orbits | degrees | rad/s | Joules |

a)

| Test B | $t_s$ $(\gamma \leq 5^o)$ | $\gamma$ acc. | $\|{}^p\boldsymbol{\Omega}_{\text{po}}\|$ acc. | Energy spent |
|---|---|---|---|---|
| Mean | 1.6529 | 1.8307 | $3.6035 \times 10^{-5}$ | $2.5768 \times 10^5$ |
| Std. dev. | 1.0631 | 0.11345 | $8.3629 \times 10^{-6}$ | $2.2591 \times 10^4$ |
| Worst case | 4.2954 | 1.9853 | $4.8376 \times 10^{-5}$ | $2.9730 \times 10^5$ |
| Units | orbits | degrees | rad/s | Joules |

b)

Table 1.7.4 — Simulation results: a) test A; b) test B.

Fig. 1.1 depicts a simulation showing $\gamma$ being reduced from $60^o$ to less then $5^o$ in only 3 orbits while controlling the satellite's spin (around the boom axis).These are encouraging results since the actuator restrictions are quite severe. However, the dissipated energy is large, as is the on-board computational power required.

## 1.8 Attitude Determination without Sensor Redundancy

## 1.9 Summary

# References

Hughes, P. (1986). *Spacecraft Attitude Dynamics.* Wiley, New York.

Krasovskii, N. (1963). *Problems of the Theory of Stability of Motion (Russian), English translation.* Stanford University Press.

Ong, W. T. (1992). Attitude determination and control of low earth orbit satellites.

Paulo Tabuada, Pedro Alves, P. T. and P. Lima (1999, September). A predictive algorithm for attitude stabilization and spin control of small satellites. In *European Control Conference - ECC'99, Karlsruhe, Germany.*

Steyn, W. H. (1994, July). Comparison of low-earth-orbit satellite attitude controllers submitted to controllability constraints. *Journal of Guidance, Control, and Dynamics 17*(4).

Wertz, J. (1990). *Spacecraft Attitude Determination and Control.* Kluwer Academic Publishers.

Wisniewski, R. (1997). *Satellite Attitude Control Using Only Electromagnetic Actuation.* Ph. D. thesis, Dept. of Control Engineering, Aalborg University.